# Slow modes in local polymer dynamics

K. Karatasos[a] and D. B. Adolf[b]
*Department of Physics and Astronomy, University of Leeds, LS2 9JT Leeds, United Kingdom*

(Received 25 January 2000; accepted 22 March 2000)

Molecular dynamics simulations of united atom nonentangled linear polyethylene models were utilized in order to systematically examine local orientational dynamics. In agreement with recent experiments and theoretical predictions, slow relaxation processes associated with motions of length scale of the order of chain dimensions are identified and analyzed with a method that allowed a model-free determination of their relative contribution to local orientational relaxation. Factors of intra- and intermolecular nature affecting their characteristics are discussed as well. © *2000 American Institute of Physics.* [S0021-9606(00)52119-9]

## I. INTRODUCTION

Polymer dynamics covers a broad range of time scales associated with length scales extending from local (of the order of a bond) to global chain dimensions. The well-known Rouse model[1] in its original or in generalized forms is commonly employed to account for dynamics in the melt state in chain lengths below the entanglement regime. Although it was shown to successfully describe global chain motion, it has been proved inadequate to account for shorter scale dynamics.[2,3] In this length scale, the Gaussian assumption ceases to be valid while details on local structure start playing a significant role.[4–6] Attempts for a more accurate description of local dynamics incorporated the effects of local chain stiffness as shorter length scales were approached. In the rotational states model[7] the characteristic ratio $C_\infty$ becomes mode dependent, while in another approach (see Refs. 8 and 9) local stiffness is modeled in terms of bending elasticity. From the experimental point of view, recent investigations revealed composite local dynamic spectra best described as the superposition of distinct relaxation processes. In Ref. 6, the model invoked for an improved description of neutron scattering data resulted in a two-mode relaxation spectra for the dynamic structure factor in nonentangled linear chains. In nuclear magnetic resonance (NMR) measurements,[10] a satisfactory fit for $T_1$, $T_{1\rho}$, and NOE (Nuclear Overhauser Effect) data assumed a two-process relaxation mechanism for the reorientation of the C–H vector in linear nonentangled polyethylene melts. These additional processes observed in local dynamics appear to reflect contributions from longer length-scale (slower) motional mechanisms. Comparison between molecular dynamics simulations in nonentangled alkanes and calculations based on a coupling scheme of the generalized Rouse eigenmodes[11] showed that the slowest first-order mode is significant for the correction of local relaxation times. Another approach (Ref. 12) is based on the dynamically disordered Rouse model,[13] where correlation functions corresponding to local motions are approximately described through the high order (i.e., shortest-wavelength) modes. It was found that low frequency contributions associated with terminal relaxation appeared in the local (segmental) spectra.

In order to address the issue of the emergence and the relative contribution of slower relaxation processes in local orientational dynamics, we performed a series of computer simulations of linear PE models. For a complete picture, this study covered dynamics in a broad range of length scales extending up to global chain dimensions.

## II. SIMULATION AND ANALYSIS METHOD

Molecular dynamics (MD) simulations of linear united atom ($CH_2$ groupings) polyethelene models were performed for chain lengths below ($N=20$) and close[14] ($N=100$) to the entanglement length. Comparison between different lengths aimed to elucidate intramolecular effects, while modifications of intermolecular origin were investigated through systematic density changes. Table I summarizes the characteristics of the simulated systems. Starting configurations were generated and equilibrated initially following the cooperative motion Monte Carlo algorithm.[15] Details on the simulation parameters as well as the static and conformational properties of these systems are discussed elsewhere.[16] Subsequently, after an additional 4 ns equilibration in the *NVT* ensemble at $T=400$ K (well above the glass transition temperature $T_g$), trajectories of 18 ns were obtained from MD runs under the *NVE* ensemble. Configurations were stored every 1 ps.

Chain segment reorientational dynamics were investigated by means of $P_2$ (second Legendre polynomial) autocorrelation functions (ACFs) of the unit vectors in the directions of the chords $\mathbf{c}_k$, connecting $k$ successive bonds along the chain contour. According to this coarse-graining scheme, $\mathbf{c}_1$ lies on the direction of a single bond, while $\mathbf{c}_{N-1}$ is on the direction of the end-to-end vector of a chain of $N$ united atoms.

For a model-independent approach on the analysis of dynamic spectra, the corresponding correlation functions, *C(t)*, were described as a continuous distribution of exponential processes[17] according to the expression

[a]Electronic mail: kkaratas@ulb.ac.be
[b]Electronic mail: D.B.Adolf@leeds.ac.uk

 

TABLE I. Characteristics of the simulated systems.[a]

| Code | Density (g/cm$^3$) | Number of chains | Chain length |
|---|---|---|---|
| $S_1$ | 0.29 | 50 | 20 |
| $S_2$ | 0.59 | 50 | 20 |
| $S_3$ | 0.70 | 50 | 20 |
| $L_1$ | 0.29 | 10 | 100 |
| $L_2$ | 0.59 | 10 | 100 |
| $L_3$ | 0.79[b] | 10 | 100 |

[a]All the systems were simulated using the Steele (Ref. 24) torsional potential.
[b]Accounts for bulk polyethylene density at $T=400$ K (Ref. 25).

$$C(t)=\int_0^\infty F[\ln(\tau)]e^{-t/\tau}d\ \ln\ \tau, \tag{1}$$

where $F[\ln(\tau)]$ symbolizes the normalized distribution of relaxation times (DRTs). Information regarding the existence of distinct relaxation processes and the dispersion of exponential decays describing each process is extracted from the number and the width of the peaks appearing in the DRTs, respectively. A characteristic time (CT) for the $i$th process appearing in the spectra can be calculated by the most probable relaxation time, denoted by the location of the maxima of the corresponding peak in the DRT.

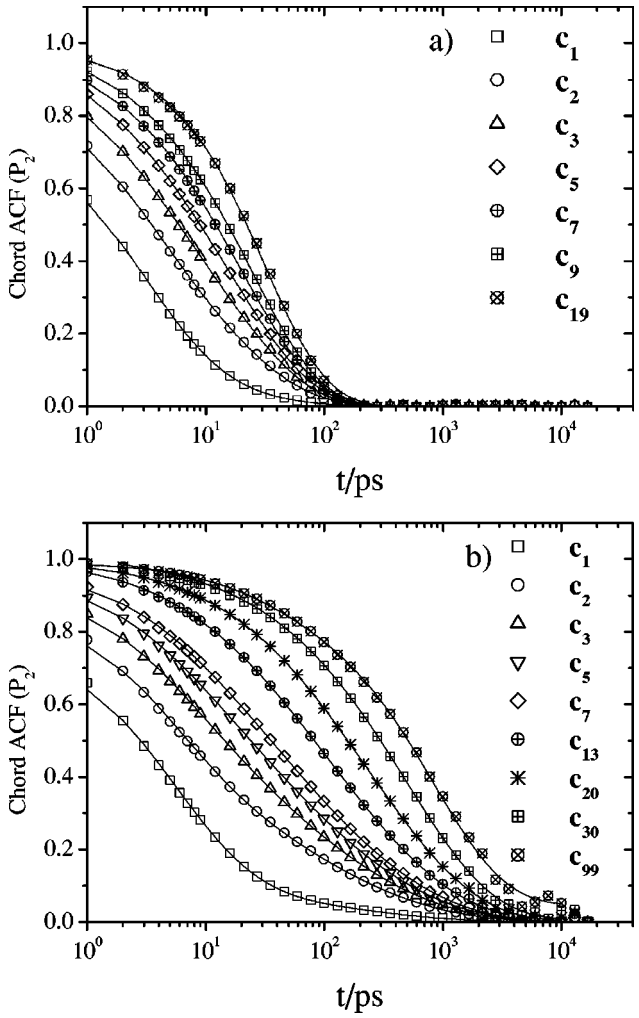


FIG. 1. $P_2$ autocorrelation function for unit chord vectors of systems $S_2$ (a) and $L_2$ (b). $\mathbf{c}_k$ vectors for high $k$ values are not shown for clarity. The solid lines through the points denote the fit resulted when utilizing Eq. (1).

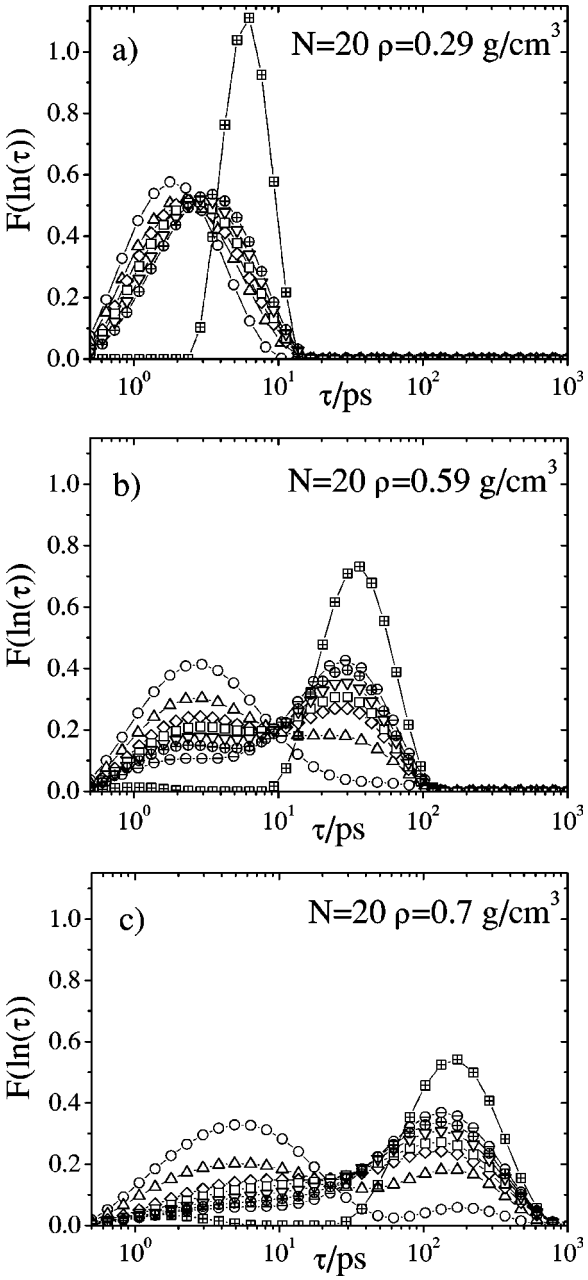


FIG. 2. DRTs for systems (a) $S_1$, (b) $S_2$, and (c) $S_3$. $\mathbf{c}_1$ (○), $\mathbf{c}_2$ (△) $\mathbf{c}_3$ (◇), $\mathbf{c}_4$ (□), $\mathbf{c}_5$ (▽), $\mathbf{c}_6$ (⊕), $\mathbf{c}_7$ (⊖),**e-e** vector (⊞). DRTs for intermediate vectors $c_k$ ($20>k>7$) are not shown for clarity. The estimated error on each point does not exceed the symbol size.

## III. RESULTS AND DISCUSSION

Figure 1 presents the $P_2$ ACFs produced by following the coarse-graining procedure described before for systems of both lengths [Fig. 1(a) for $S_2$ and Fig. 1(b) for $L_2$] at the same density of $\rho=0.59$ g/cm$^3$. The longest chord corresponds to the end-to-end vector. As depicted in Figs. 1(a) and 1(b), starting from the $\mathbf{c}_1$ ACF which describes the reorientation of a single bond, the longer chords' ACFs approach the end-to-end vector behavior in a rather continuous

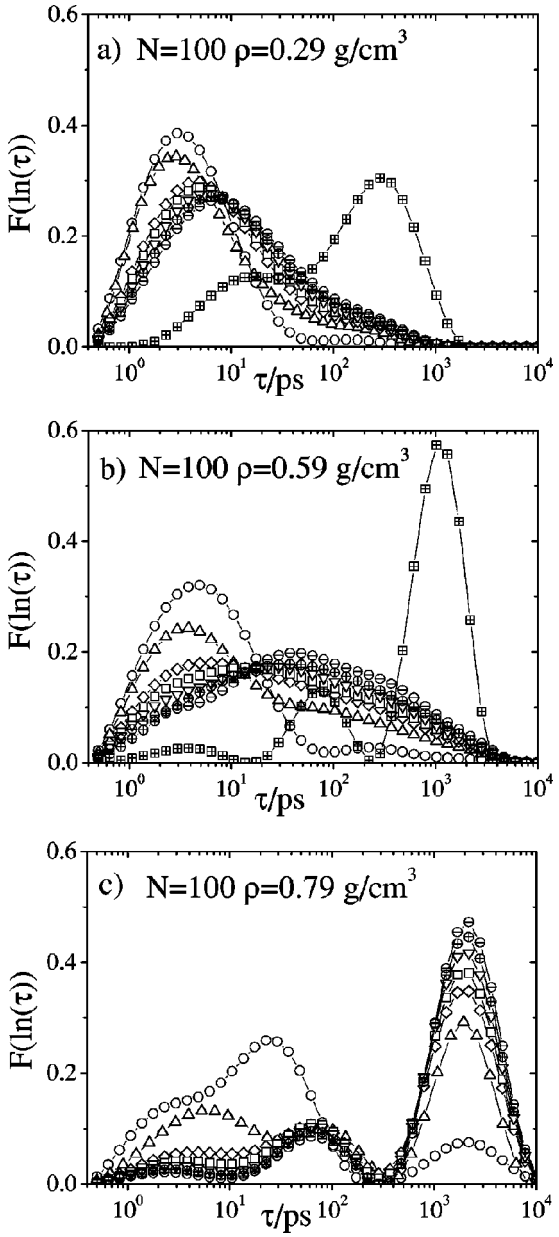


FIG. 3. DRTs for systems (a) $L_1$, (b) $L_2$, and (c) $L_3$. $c_1$ (○), $c_2$ (△), $c_3$ (◇), $c_4$ (□), $c_5$ (▽), $c_6$ (⊕), $c_7$ (⊖), **e-e** vector (⊞). DRTs for intermediate vectors $c_k$ ($100>k>7$) are not shown for clarity. The estimated error on each point does not exceed the symbol size.

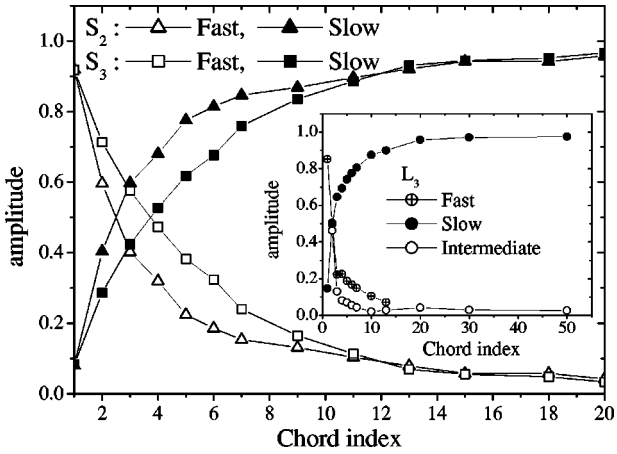


FIG. 4. Relative amplitudes of the two processes for systems $S_2$ [slow (■), fast (□)], and $S_3$ [slow (▲), fast (△)]. Inset: Relative amplitudes of the three processes describing the $L_3$ system [slow (●), intermediate (○), fast (⊕)]. The estimated errors are of the size of the symbols. Lines connecting the points are guides to the eyes.

manner in terms of shape variation. Distributions of relaxation times[18] $F[\ln(\tau)]$ of $P_2$ ACFs for the short length systems $S_1$, $S_2$, $S_3$ are shown in Figs. 2(a), 2(b), and 2(c), respectively. At the lowest density [Fig. 2(a)], a single process is observed. The peak location is shifted to longer times as the chord length increases toward the end-to-end vector. At the intermediate [Fig. 2(b)] and the higher [Fig. 2(c)] density, a double-peaked distribution is clearly resolved. At constant density, the temporal separation between the fast and the slow process (as can be visualized by the time difference of the two maxima) remains approximately constant for all the chord vectors, while their peak locations practically coincide with the characteristic times for the reorientation of the bond and the end-to-end vector, respectively. The splitting of the DRT is already apparent from the bond spectra of the denser system and the $\mathbf{c}_2$ of the intermediate density [Figs. 2(b) and 2(c)]. Figure 3 illustrates the DRTs corresponding to the $\mathbf{c}_k$ vectors' ACFs for systems $L_1$, $L_2$, $L_3$. At the lowest density [Fig. 3(a)] the DRTs describing reorientation of the short-length chords show a single but progressively broader peak which is shifted to longer times as the chord length increases. A long time tail develops when increasing the chord index of the examined vectors and a two-peaked end-to-end vector spectra is observed. The DRTs of the intermediate density [Fig. 3(b)] are more complex. In this case, a three-peak structure is the final result of the modes' evolution. A fast process on the time scale of the bond's reorientation possess the smallest amplitude, an intermediate process of moderately higher amplitude, and a slow dominant process describing the longer length-scale relaxation.

At the higher density system [Fig. 3(c)] the triple-peak structure already appears from the $\mathbf{c}_2$ spectra and persists to the longer chords. The relaxation distribution for the end-to-end vector is not calculated since the corresponding $P_2$ ACF decorrelates only to a small extent in our time window. Nevertheless, based on the behavior of the shorter chords' ACFs, it is expected that the DRT related to the end-to-end vector would exhibit similar characteristics. The most prominent feature emerging from the longer systems' spectra is the appearance of the intermediate process occurring on the same time scale for the $L_2$ and $L_3$ systems.

The dual character of the DRTs for the short chain systems far above the $T_g$ temperature indicates that reorientation on any length scale can actually be described by means of contributions associated with two characteristic time scales—one for the reorientation of the bond (commonly identified as the segmental time scale[19–21]) and one for the end-to-end vector. However, for longer (but still unentangled) chains, the proximity to the entanglement regime seems to affect local dynamics. Recent NMR experiments[10] in a melt PE sample of 153 carbon atoms revealed that intermediate time-scale dynamics between the fast (segmental)

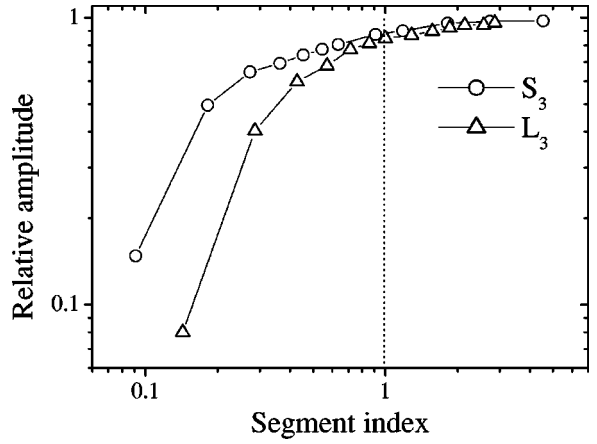


FIG. 5. Relative amplitudes for the slowest modes in systems $L_3$ (○) and $S_3$ (▽). The vertical dotted line denotes the length of one statistical segment.

and the very slow global chain motion are important for describing the C–H vector reorientation. This observation is consistent with the appearance of the intermediate process for the long chain/high density systems $L_2$ and $L_3$. Its absence from the shorter chain spectra and the fact that its CT remains practically unaltered when two different densities and various chord lengths are examined suggests that it may be related to a characteristic length/time scale in the pre-entanglement regime.

A quantitative account of the evolution and the relative contribution[22] of the related processes in the DRT spectra is presented in Fig. 4. As evidenced by the dependence of the respective amplitudes when advancing from the bond toward the end-to-end vector, an interchange of the relative contribution between different processes takes place. Namely, the amplitude of the slower process is systematically enhanced at the expense of the faster modes. The increase of density at constant length promotes relaxation through the slower channels. The amplitude of the slow process in system $S_3$ ($\rho=0.70$ g/cm$^3$) increases at a higher rate than in system $S_2$ ($\rho=0.59$ g/cm$^3$). The behavior in the long chain system $L_3$ (the inset of Fig. 4) is similar to the short length models. It must be noted, though, that the ''amplitude transfer'' toward the slower process is realized via both the fast and the intermediate modes. A point that should be emphasized for systems $S_2$ and $S_3$ is that for both densities the relative amplitudes of the slow modes assume similar values from vector $\mathbf{c}_9$ and onwards. This vector describes reorientation in the length scale of a statistical segment.[23] In other words, the relative amplitude of the slow mode becomes insensitive to density for longer length scales. To further elaborate on this concept, Fig. 5 shows a comparison of the amplitudes of the slowest modes in systems $L_3$, $S_3$ when the length scale is mapped in terms of the segment (instead of the chord) index.

Figure 5 illustrates that the previously observed behavior is valid for both chain lengths. In addition, it is apparent that there can be no single power law dependence of the amplitude on the segment index which describes both length-scale regimes below and above a statistical segment.

In summary, it was found that the appearance of long length-scale modes in local reorientational spectra is a combined effect of inter- (density comparisons) and intra- (chain length comparisons) molecular origin. At high densities the slowest process contributes appreciably in the loss of orientation at length scales down to the scale of a bond. Its CT is of the order of the time scale for global chain reorientation. The corresponding amplitude shows the most significant increase when advancing from a single bond toward vectors describing reorientation in lengths below the statistical segment. Its behavior for longer length scales becomes virtually independent of density and chain length. The intermediate process in the local reorientational spectra solely for the long chain models emphasizes the different configurational/topological characteristics between the short and long chain systems.

Although the above-mentioned description refers to polyethylene models, it is expected to form a common basis for reorientational dynamics of linear chains with similar flexibility.

[1] P. Rouse, J. Chem. Phys. **21**, 1272 (1953).
[2] M. Mondello, G. Grest, E. Webb, and P. Peczak, J. Chem. Phys. **109**, 798 (1998).
[3] W. Paul, G. Smith, D. Yoon, B. Farago, S. Rathgeber, A. Zirkel, L. Willner, and D. Richter, Phys. Rev. Lett. **80**, 2346 (1998).
[4] Z. Reiner, T. Kanaya, T. Kawaguchi, D. Richter, and K. Kaji, J. Chem. Phys. **105**, 1189 (1996).
[5] T. Kanaya, T. Kawaguchi, and K. Kaji, Macromolecules **32**, 1672 (1999).
[6] D. Richter, M. Monkenbusch, J. Allgeier, A. Arbe, J. Colmenero, B. Farago, Y. Bae, and R. Faust, J. Chem. Phys. **111**, 6107 (1999).
[7] G. Allegra and F. Ganazolli, J. Chem. Phys. **74**, 1310 (1981).
[8] L. Harnau, R. Winkler, and P. Reineker, J. Chem. Phys. **106**, 2469 (1997).
[9] L. Harnau, R. Winkler, and P. Reineker, Europhys. Lett. **45**, 488 (1999).
[10] X. Qiu and M. Ediger, Macromolecules **33**, 490 (2000).
[11] K. Kostov, K. Freed, E. Webb, M. Mondello, and G. Grest, J. Chem. Phys. **108**, 9155 (1998).
[12] B. Ilan and R. Loring, Macromolecules **32**, 949 (1999).
[13] R. Loring, J. Chem. Phys. **108**, 2189 (1998).
[14] The length of $N=100$ of systems $L_1$, $L_2$, $L_3$ is below the entanglement length of $N=138$ reported for a similar system at $T=509$ K [see Richter *et al.*, Macromolecules **27**, 7437 (1994)], however it is expected to be in the proximity of the corresponding $N_e$ at the examined temperature.
[15] T. Pakula, J. Chem. Phys. **95**, 4685 (1991).
[16] K. Karatasos, D. Adolf, and S. Hotston, J. Chem. Phys. **112**, 8695 (2000), this issue. The force field used is based on Brown *et al.*, *ibid.* **104**, 2078 (1996).
[17] Here we essentially adopt the so-called ''heterogeneous'' picture [see, for instance, Richter *et al.*, Phys. Rev. Lett. **82**, 1335 (1999), and references therein], where local relaxation processes are expressed as a superposition of single exponentials weighted by a distribution of relaxation times $F[\ln(\tau)]$.
[18] All the DRTs presented henceforth are chosen among almost identical, in terms of spectral characteristics (number, location, and shape of the peaks), solutions for $F[\ln(\tau)]$ [see Eq. (1)] possessing the minimum degree of information (i.e., number of peaks) absolutely necessary to describe the data.
[19] H. Takeuchi and R. Roe, J. Chem. Phys. **94**, 7446 (1991).
[20] R. Roe, J. Non-Cryst. Solids **172–174**, 77 (1994).
[21] A. Kopf, B. Dunweg, and W. Paul, J. Chem. Phys. **107**, 6945 (1997).
[22] Calculated from the area under a peak, obtained as the zeroth moment of the solution referred to this peak.
[23] Segment lengths as estimated through the characteristic ratio $C_n=\langle R^2\rangle/(nl^2)$ ($R$ is the end-to-end distance, $n$ the number of bonds per chain, and $l$ the bond length) for each system, where $s_{L3}\simeq 11$ bonds and $s_{S3}\simeq 7$ bonds.
[24] D. Steele, J. Chem. Soc., Faraday Trans. 2 **81**, 1077 (1985).
[25] R. Raff and J. Allison, *Polyethylene* (Interscience, New York, 1989).